UNIVERSITY OF LEEDS

This is a repository copy of *A small-molecule acts as a 'roadblock' on DNA, hampering its fundamental processes*.

White Rose Research Online URL for this paper:
http://eprints.whiterose.ac.uk/121717/

Version: Accepted Version

eprints@whiterose.ac.uk
https://eprints.whiterose.ac.uk/

A small-molecule acts as a 'roadblock' on DNA, hampering its fundamental processes

Amit Kumar*[a,b]

[a]Astbury Centre for Structural Molecular Biology, School of Molecular and Cellular Biology, University of Leeds, Leeds LS2 9JT, UK.

[b]Institute of Physics, Biophysics, Martin–Luther–University Halle–Wittenberg, Germany

E-mail: A.Kumar@leeds.ac.uk

Highlight:

-Zn^{2+} complex interacted with the grooves of DNA

-Zn^{2+} complex interacts without inducing conformational changes or exhibiting chemical nuclease activity

-DNA binding of Zn^{2+} complex hampers ('roadblock') walking of DNA-moving protein e.g. DNA polymerase

-DNA roadblock phenomenon exhibited at DNA which resulted in reduced contents of both RNA and protein

- Roadblock of DNA led to growth inhibition of pathogenic bacteria

-----

-Zn^{2+} complex interacted with the grooves of DNA

-Zn^{2+} complex does not induce conformational changes or exhibit chemical nuclease activity

-Zn^{2+} complex hampers ('roadblock') walking of DNA-moving protein e.g. DNA polymerase

-DNA roadblock phenomenon exhibited at DNA, resulted in reduced contents of RNA and protein

- Roadblock of DNA led to growth inhibition of pathogenic bacteria

Abstract:

DNA replication, RNA and protein synthesis are the most fundamental housekeeping processes involved in an organism's growth. Failure or dysregulation of these pathways are often deleterious to life. Therefore, selective inhibition of such processes can be crucial for the inhibition of the growth of any cell, including cancer cells, pathogenic bacteria or other deadly microbes. In the present study, a Zn^{2+} complex is shown to act as a roadblock of DNA. The Zn^{2+} complex inhibited DNA taq polymerase activity under the in vitro conditions of PCR. Under in vivo conditions, it readily crosses the cell wall of gram-negative bacteria (E. coli), leading to the reduction of RNA levels as well as protein content. Growth of pathogenic bacteria (e.g., Staphylococcus aureus and Pseudomonas aeruginosa) was also significantly retarded. The Zn^{2+} complex binds to the grooves of the DNA without inducing conformational changes or exhibiting chemical nuclease activity. To the best current knowledge, this is first coordination complex exhibiting a 'roadblock' property under both in vitro and in vivo conditions (show at all three levels – DNA, RNA and protein). The label-free approach used in this study may offer an alternative route towards fighting pathogenic bacteria or cancer cells by hampering fundamental cellular processes.

Introduction

In cancer cells, most metabolic rates are higher than those found in healthy cells, including fundamental housekeeping processes such as DNA replication, repair and fragmentation [1]. DNA and DNA binding proteins are pivotal to most biochemical processes. For example, RNA polymerase and other factors bind to DNA, resulting in RNA synthesis and eventually protein synthesis. These proteins, in turn, regulate the organisms' growth by participating in biochemical reactions. Therefore, DNA-binding proteins play an essential and critical role in cell growth and development, as they control fundamental biochemical activities including DNA replication and transcription. Therefore, selective inhibition of such processes involving housekeeping proteins can be crucial for the inhibition of growth of any type of cell, including cancer cells, pathogenic bacteria or other deadly microbes [2-4].

There is a continuous effort to develop small molecules, including metal-based coordination complexes, for oncotherapy as well as novel anti-microbial agents [5-8]. Since the discovery of the cisplatin/carboplatin, several coordination complexes without platinum have been synthesized for improved reactivity and activity against broad range of cancer cells[7]. The properties of coordination complexes, such as the metal centre and the organic skeletal of the ligand, can be tuned to suit the desired biological activity. Recently, pyridine-based metal complexes have been developed for DNA binding [9] and thus may act as blockers of DNA-binding/walking proteins [9], inhibiting important biological processes including DNA polymerization [7]. Recently, Yu et al. showed inhibition of Taq polymerase function during PCR using a Ruthenium-based polypyridyl complex [10] and Chandra et al. using Iridium complexes [11]. Many of the currently developed coordination complexes exhibited cytotoxicity under in vitro conditions with either an apoptotic mode of action, or more often with an unknown mechanism, without knowing their cellular targets [12]. However, it is of medical interest to find coordination

complexes/small molecules which are able to cross the cell wall/membrane barrier and exhibit cell toxicity by targeting the biomolecules responsible for specific housekeeping pathways [5, 13].

Redox stability, variability in coordination chemistry and reduced metal toxicity makes Zn(II) one of the most common metal ions found in biological systems [14, 15]. Zn-based coordination compounds have been studied for various activities, including toxicity toward infectious organisms [16]. They exhibit more specific functions, such as the inhibition of caspase-3 activity and promotion of ErbB1-ErbB2 heterodimerization by Zinc pyrithione [17], inhibition of cyclin-dependent kinase CDK1 [18]and inhibition of parathyroid hormone activity [13]. Induction of phosphorylation of the Akt downstream effector glycogen synthase kinase 3β and thus proposed to serve as lead structures for developing antidiabetic drugs and useful tools for regulating glucose metabolism to name but a few examples [19]. Zn^{2+} complexes are also known to exhibit antibacterial/antimicrobial, anticancer activities, interacting with DNA and the inducing protein aggregation [20-26].

In the present study, a water-soluble coordination complex of Zn(II) and anthracenyl terpyridine (Figure 1 and S1) [6, 13] has been employed as a roadblock of DNA preventing polymerase activity. The Zn^{2+} complex inhibited DNA taq polymerase activity under the in vitro conditions of PCR. Under in vivo conditions, it readily crosses the cell wall barrier of gram-negative bacteria (E. coli), leading to the reduction in RNA as well as protein content.

Results

Interaction of Zn^{2+} complex to DNA

The fundamental aspect of working as a barrier is a physical interaction with DNA [6, 8, 27]. A fluorescent dye displacement method can be utilized to evaluate the mode of binding. Propidium iodide and Hoechst 33258 were chosen as intercalating and groove (minor)-binding dyes, respectively [6]. These dyes have minimal fluorescence when free in aqueous solution. Their fluorescence intensity enhances several-fold once they bind to nucleic acids. Consequently, upon addition of the dye to dsDNA, a significant enhancement in their fluorescence intensity was observed. Gradual addition of the Zn^{2+} complex to a solution containing DNA and propidium iodide leads to a marginal decrease in fluorescence intensity. This shows that the Zn^{2+} complex was not intercalating with the dsDNA. The Zn^{2+} complex was able to displace 20-30 % of the propidium iodide intercalated to DNA. On the other hand, addition of the Zn^{2+} complex significantly diminishes Hoechst 33258 fluorescence intensity. Further analysis suggested that the Zn^{2+} complex is able to displace the Hoechst 33258 up to 80-90 % (Figures 1B and 1C). The results clearly indicated that Zn^{2+} complex interactions occur at the groove of the dsDNA. As a control molecule, 9-anthracene methanol or Zn^{2+}-perchlorate were incubated with the DNA, with neither able to displace either dye (Figures 1C and S2). Absorption studies provide further evidence for the Zn^{2+} complex interaction with DNA. A fit of the data obtained a K_D of 2.7 µM (Figure 1 D and S3). Previous results indicated that replacement of the Zn^{2+} with Cu^{2+} completely changes the binding mode of the coordination complex. The Cu^{2+} complex bearing the same organic skeletal system binds to the dsDNA via intercalation [6], in contrast to the groove-binding Zn^{2+} complex herein. The binding mode of the complex is thus directed by the metal ion. The central metal ion might

reinforce binding affinity with the negatively charged phosphate groups of DNA via electrostatic interactions. Additional molecular interactions are contributed by the organic skeletal system to displace Hoechst 33258.

Inhibition of DNA polymerase activity during PCR

In general, the grooves of the DNA expose the most functional groups to biomolecules, hence most biological activity takes place at these sites via the recognition of specific sequences to DNA-binding proteins [28]. With the understanding of the groove-binding nature of the Zn^{2+} complex, 'roadblock' activity was investigated during PCR using Taq polymerase. The complete PCR mixture containing plasmid DNA, primers, dNTPs, DNA polymerase, suitable buffer for enzyme activity and an increasing amount of the Zn^{2+} complex, was run for 30 cycles. The PCR products were analysed by 1 % agarose gel electrophoresis. The band intensity on the agarose gel could be directly correlated with 'roadblock' activity. A gradual decrease in the PCR product was observed with an increasing amount of the Zn^{2+} complex (Figures 2 A – C). The IC_{50} value (concentration at which the PCR product was equal to 50 % of PCR product where no Zn^{2+} complex was added) of the Zn^{2+} complex was found to be 9.23 ± 1.78 µM. Neither 9-anthracene methanol nor Zn^{2+}-perchlorate had any effect on the polymerase activity (Figure S4A). To confirm that the Zn^{2+} complex is not inhibiting the Taq polymerase directly, but instead the origin of roadblock activity is arising due to DNA binding, a 5-fold excess of Taq polymerase was added, keeping the other parameters constant. At this high concentration, no PCR product was observed (Figure S4B). This finding confirms that the origin of roadblock activity is due to DNA binding, not by inhibition of enzyme activity.

Roadblock activity does not alter DNA's conformations

Often, the addition of small molecules bearing hydrophobic moieties to the DNA induces conformational changes in the latter [6]. Therefore, CD spectra were recorded in the presence and absence of Zn^{2+} complex. No significant changes in DNA conformation were observed by CD spectroscopy (Figure 3A) when titrated against the Zn^{2+} complex. Small coordination molecules which intercalate DNA are known to induce such conformational changes [6]. The Zn^{2+} complex, studied here however, binds to the grooves and is thus unable to induce sufficient conformational changes. It is thus impossible that the loss of enzyme activity originates from a ligand-induced conformational change preventing DNA binding of Taq polymerase. Additionally, melting temperature (T_m) measurements of DNA suggested an increase in the T_m by 3.8 °C in presence of Zn^{2+} complex (Figure 3B). Whereas 9-anthracene methanol has a negligible effect on DNA melting. Free Zn(II) is known to decrease in the T_m of DNA [29].

Roadblock activity does not arise by chemical nuclease activity

Often, coordination complexes, including those of Zn^{2+}, exhibit chemical nuclease activity when incubated with DNA[6]. Therefore, the nuclease activity of the Zn^{2+} complex was analysed at 37 °C using a pET plasmid. No nuclease activity was observed under these conditions (Figure 4, left hand side). Additionally, chemical nuclease activity was also tested under PCR conditions for 30 cycles (see Methods). Again, no change in plasmid DNA content was observed (Figure 4, right hand side). These experiments thus provide further evidence that roadblock activity is solely due to the binding of the Zn^{2+} complex to the DNA.

Exhibition of roadblock activity under in vivo conditions

The roadblock property can be utilized to inhibit the movement of DNA-binding proteins along the helical strand, which controls important cellular processes. To investigate the effect of the roadblock property under in vivo conditions, the level of transcription in E. coli was assessed. During transcription, a portion of the double-stranded DNA template produces a single-stranded RNA molecule. Several proteins, including RNA polymerase and various transcription factors bind to the DNA and transcribe the complementary RNA from the gene [30]. In growing cells, transcription is a housekeeping process, with RNA molecules continuously produced inside the cell. To evaluate this experimentally, E. coli cells were transformed with a pET15b vector containing the p19^{INK4d} gene under the T7 promoter (an IPTG-inducible promoter). These cells were grown with an increasing amount of Zn^{2+} complex, followed by IPTG-induction. It was hypothesized that due to the quick doubling time of the bacteria, cells will try to produce RNA molecules for various cellular activities. Also, due to the IPTG-induction step, cells will be producing mRNA continuously. If the Zn^{2+} complex is indeed working as a roadblock for DNA-binding proteins, then there should be a concomitant decrease in RNA content with an increasing amount of Zn^{2+} complex. RNA quantification showed that there is a gradual decrease in the RNA content with respect to the Zn^{2+} complex (Figure 5A and S5). The Zn^{2+} complex exhibited an IC$_{50}$ of 15.5 ± 1.5 µM (where 50 % of RNA content can be detected) (Figure 5A). The IPTG-induced over-expression was used as both an easy read-out of roadblock activity and to reduce the background noise of other cellular RNAs. These experiments clearly demonstrated the roadblock property of the Zn^{2+} complex at the RNA level under in vivo conditions. The Zn^{2+} complex may have showed toxicity at higher concentrations upon longer incubation; expected due to the roadblock

activity and other possible phenomenon. Therefore, an equal amount of cells, monitored by OD_{600nm}, were disrupted and loaded onto the gel.

An additional readout of the roadblock property can be demonstrated at the protein level. Here, E. coli cells transformed with a pET15b vector containing the $p19^{INK4d}$ gene under the T7 promoter were used. The cells were grown in the presence of the Zn^{2+} complex and induced with IPTG as described above. After 6 h incubation, an equal amount of protein (determined by the Bradford assay) was loaded onto the SDS-PAGE gel. Band intensities at ~19 kDa showed a marked reduction in protein content with respect to the Zn^{2+} complex (Figure 5B and S6). The IC_{50} value was found to be 15.57 ± 3.35 µM. It is interesting to note that the IC_{50s} obtained at the RNA level and protein levels coincide with one other. These results clearly demonstrated that the Zn^{2+} complex showed DNA roadblock activity at the RNA level, which directly reflects at the protein level.

The Zn^{2+} roadblock inhibits pathogenic bacterial growth:

Next, the significance of roadblock activity was analysed against the pathogenic bacteria Staphylococcus aureus (gram-positive) and Pseudomonas aeruginosa (gram-negative) as chosen from the 'ESKAPE pathogens' category[5, 16, 31]. The IC_{50} was found to be 9.0 ± 0.2 µM and 8.65 ± 0.7 µM for Staphylococcus aureus and Pseudomonas aeruginosa, respectively (Figure 6). The results indicate that the Zn^{2+} complex is able to inhibit the growth of pathogenic bacteria.

Discussion:

The emergence of multi-drug resistant strains of bacteria is one of the biggest threats to human health. Pathogenic bacteria of the 'ESKAPE category' are of particular concern. Among this category 'KAPE' are the gram-negative bacteria which are more likely to attain multi-drug resistance compared to gram-positive organisms [31]. Studies have suggested that by 2050, the continuous rise in antimicrobial resistance could account the death of 10 million people each year [32]. The discovery of drug molecules which act against gram-negative bacteria is often challenging. Gram-negative bacteria possess an outer polysaccharide layer and multi-drug efflux transporters, which render many small molecules, including antibiotics eventually ineffective. Drug resistance phenomena have drawn the focus of drug-discovery towards a novel, distinct class of molecules than the ineffective small molecules which currently exist. Research groups have paid attention towards the development of water-soluble, metal-based coordination molecules which can cross the cell wall/membrane and can target the crucial housekeeping biochemical pathways of organisms. Coordination complexes have been shown to exhibit antimicrobial [33, 34], antifungal [35-37] and anticancer [6, 7] activities and therefore applied in industry, ecology, or medicine.

Housekeeping bio-processes such as DNA, RNA and protein synthesis control the growth of the organism. Inhibition of these pathways is deleterious and often results in the organism's death. The presented Zn^{2+} complex interacts at the groove of the DNA without inducing conformational changes or chemical nuclease activity. It is well known that DNA's grooves expose more functional groups, allowing sequence-specific DNA-binding proteins to recognize them [28]. As a consequence of Zn^{2+} complex binding, retardation in the DNA polymerization process was observed under PCR conditions. RNA polymerization is yet another result of walking of the specific proteins over the

DNA strand. The Zn^{2+} complex has inhibited these pathways through interactions with DNA under in vivo conditions inside bacteria. As a consequence a reduction in protein content was also observed. Thus, the Zn^{2+} complex has blocked the pathways of the proteins moving along the DNA helix under both in vitro and in vivo conditions. Once the fundamental housekeeping bioprocesses are blocked, the consequences are potentially lethal to pathogenic bacteria, as shown for Staphylococcus aureus and Pseudomonas aeruginosa.

Small molecules such as nalidixic acid, ciprofloxacin and norfloxacin can inhibit DNA synthesis. Quinolones are known to act upon DNA gyrase as topoisomerase inhibitors, inhibiting DNA polymerization [38]. Other examples such as rifampin, an RNA polymerization inhibitor, which acts upon DNA-dependent RNA polymerase [39]. These molecules directly inhibit the function of protein molecules involved in DNA/RNA polymerization, rather than by blocking the procession of DNA-binding proteins along the helical strand by direct interaction with DNA. Several coordination molecules exist which exhibit interaction with DNA as well as chemical nuclease activity [6-8]. Often these molecules showed anticancer or antibacterial activities. The anticancer activity sometimes resulted from apoptotic cell death or an unknown mechanism; the latter more often the case with bacteria. Also, under such circumstances, a coordination complex's specific cellular targets remain elusive considering its complex cellular environment. The Zn^{2+} complex studied here directly interacts with the DNA, acting as a roadblock for proteins which move along the DNA. Although the Zn^{2+} complex showed roadblock activity by DNA binding, additional interactions with other cellular proteins can not be ruled out.

In summary, the DNA binding of a Zn^{2+} complex and its biological significance has been demonstrated as a roadblock for DNA polymerase. Many of the coordination complexes currently developed can barely cross the cell membrane/wall to reach their targets,

preventing their activity under in vivo conditions. The Zn^{2+} complex presented here readily crosses the cell wall of gram negative bacteria and exhibited roadblock activity. These studies are the first assessment of DNA binding by a coordination molecule which exhibits roadblock activity under in vitro and in vivo conditions. Such a 'roadblock' approach could be applied towards the inhibition of other fundamental processes carried out by DNA-binding proteins and their procession along the DNA helix. Impediment of these housekeeping processes can be deleterious to cells and thus the complex's activity could be applied to targeted therapies for the inhibition of the growth of pathogenic bacteria or carcinogenic cells.

Experimental section

UV-visible spectroscopy

Stability of the Zn^{2+} complex (at 20 µM) was analyzed by absorption spectroscopy over a 10 h time period in 25 mM Tris.HCl buffer pH 7.4. For the interaction studies, 25 µg of DNA was titrated against 8 µM of Zn^{2+} complex at each step. In the case of 9-anthracene methanol, 64 µM was added to the DNA solution and the spectrum was recorded. The data were fitted using a second order polynomial function. In these case Zn^{2+} complex or 9-anthracene methanol titrated against buffer was taken as control and subtracted from the main titration before analysis. On the other hand, in the metal ion displacement experiments, 20 µM of Zn^{2+} complex was taken and a 1:10 ratio of metal ions was added in the form of $MgCl_2.6H_2O$, $CaCl_2.2H_2O$, $MnCl_2.4H_2O$ and $FeCl_3$. The spectrum from the solution of metal ion in buffer alone was subtracted from the main experiment. Note: Zn^{2+} complex or 9-anthracene methanol were initially dissolved in dimethyl sulfoxide and further diluted for the experiments. In any experiment, [dimethyl sulfoxide] was less than 1 % (v/v).

Fluorescence spectroscopy:

Fluorescence spectroscopy experiments were performed in 25 mM Tris.HCl buffer pH 7.4. For the dye displacement experiment, calf thymus DNA was used. The reaction mixture was prepared by mixing 25 µg of DNA and 10 µl of 1 mg/ml of propidium iodide or 16 µl of 2 µg/ml of Hoechst 33258 to a total volume of 1 ml. This reaction mixture was excited at 342 nm or 352 nm for propidium iodide and Hoechst 33258, respectively. Small aliquots of Zn^{2+} complex (4 µM) were added and the spectrum was recorded after

each addition. Solution containing propidium iodide or Hoechst 33258 titrated with Zn^{2+} complex was considered as a blank titration. This blank titration was subtracted from the main titration before data analysis. All the experiments were performed on a Jasco FP6500 fluorescence spectrometer.

Polymerase chain reaction (PCR):

A standard protocol described by New England BioLabs Inc. was used for the PCR reaction. In brief, plasmid DNA (~100 ng), primers (0.2 µM each reverse and forward), dNTPs (200 µM), DNA polymerase (1.25 units) and suitable buffer were mixed together. The Zn^{2+} complex was added to give a final concentration of $0 - 100$ µM. The total reaction volume was made up to 50 µl using autoclaved water. The Taq polymerase activity was analysed for $p19^{INK4d}$, corresponding to a 498 base pair gene cloned in pET15b. The PCR reaction was carried out on a VWR thermal cycler for 30 cycles. The resulting PCR products were analyzed on a 1 % (w/v) agarose gel. The band intensity was analysed using ImageJ software.

CD spectroscopy:

Measurements were carried out using 120 µg of calf thymus DNA in 5 mM Tris.HCl buffer at pH 7.4. In a titration experiment, small aliquots of 4 µM Zn^{2+} complex were added to 1 ml of DNA solution. Spectra were recorded after each addition. Each spectrum was an average of three successive scans. The experiments were carried out on Jasco J-815 CD spectropolarimeter.

Melting temprature measurements

Melting temprature measurements were performed using absorption spectroscopy at 260 nm. The DNA samples (100 µg) in the absence or presence of 15 µM of Zn^{2+} complex or 9-anthracene methanol were heated from $0 - 100$ °C (in steps of 5 °C) in 25 mM Tris.HCl buffer at pH 7.4. The samples were incubated at each temprature measurement 5 minutes before taking the OD_{260nm}. The experiments were carried out on Jasco V 670 UV-visible spectrometer.

Chemical nuclease activity:

DNA cleavage activity of the Zn^{2+} complex was analyzed by agarose gel electrophoresis. The Zn^{2+} complex $(0 - 100$ µM) was mixed with 150 ng of pET15b, possessing the p19^{INK4d} gene. This reaction mixture was incubated at 37 °C for 3 h or in the PCR machine for 30 cycles. DNA cleavage activity was analyzed in 25 mM Tris.HCl buffer at pH 7.4.

In vivo roadblock assay:

The roadblock activity of the Zn^{2+} complex was analyzed by co-incubating it with E. coli BL21(DE3) cells. In the experiment, freshly grown E. coli BL21(DE3) cells were transformed with the pET15b vector containing the p19^{INK4d} gene under a T7 promoter (IPTG-inducible promoter). These cells were inoculated in LB media at an initial OD_{600nm} of 0.05. These cells were allowed to grow until $OD_{600nm} = 0.1$. The cells were grown at 37 °C with constant agitation at 300 rpm. Increasing amounts of Zn^{2+} complex were added and incubated for 30 minutes. After this incubation, 1 mM of IPTG was added and

further incubated for 6 h. After this incubation, equal amounts of E. Coli BL21(DE3) cells were taken (monitored by OD_{600nm}), the cells were centrifuged (7000 rpm) and the media discarded. The cell pellet was re-suspended and lysed in 200 µl of 25 mM Tris.HCl buffer at pH 7.4, containing deoxyribonuclease I and ribonuclease inhibitors. The whole cell lysate was mixed with 6x loading dye and 30 µl was loaded on a 1 % agarose gel. The gel was stained with ethidium bromide and analysed under UV light. The band intensity was analysed using ImageJ software.

To assess the roadblock activity at the protein level, E. coli BL21(DE3) cells transformed with the pET15b vector containing the p19[INK4d] gene under T7 promoter were used. The transformed cells were initially inoculated and grown until the OD_{600nm} reached $0.6 - 0.7$. The cells were grown at 37 °C with constant agitation at 300 rpm. An increasing amount of Zn^{2+} complex was added and growth continued for 30 minutes at 37 °C. After 30 minutes, the cells were induced with 1 mM IPTG and further grown for 6 h. The cells were then centrifuged and lysed (by sonication at 40 % amplitude) in 200 µl of 25 mM Tris.HCl buffer pH 7.4 containing deoxyribonuclease I and protease inhibitors. The lysate was clarified by centrifugation (12000 rpm) and the protein concentration was determined using the Bradford protein assay. An equal amount of protein was loaded onto the gel using 6x SDS loading dye and analysed on a 12 % SDS-PAGE gel. The band intensity close to 19 kDa (p19[INK4d]) was analysed using ImageJ software.

IC$_{50}$ value determination for pathogenic bacteria

For the IC$_{50}$ value determination, freshly grown Staphylococcus aureus and Pseudomonas aeruginosa cells at their log phase were used. Zn^{2+} complex with concentrations ranging from $0 - 6$ µM was added to 10 ml of nutrient broth media. These tubes were inoculated at a starting OD_{600nm} of 0.05 and incubated for 10 h at 37 °C with rotation at 300 rpm.

The OD$_{600nm}$ of the bacteria where Zn^{2+} complex was not added was considered as 100 % bacterial growth. The growth inhibition experiments were performed with three technical repeats and at least two independent experiments performed.

References

[1] C.M. O'Connor, J.U. Adams Journal (2010) Pages.

[2] C.P. Carvalho, A. Norouzy, V. Ribeiro, W.M. Nau, U. Pischel, Org. Biomol. Chem., vol. 13, 2015, pp. 2866-2869.

[3] G. Ghale, V. Ramalingam, A.R. Urbach, W.M. Nau, J. Am. Chem. Soc., vol. 133, 2011, pp. 7528-7535.

[4] P. Jagtap, C. Szabo, Nat. Rev. Drug. Discov., vol. 4, 2005, pp. 421-440.

[5] A. Kumar, J. Balbach, Sci. Rep., vol. 7, 2017, pp. 42141.

[6] A. Kumar, J.P. Chinta, A.K. Ajay, M.K. Bhat, C.P. Rao, Dalton Trans., vol. 40, 2011, pp. 10865-10872.

[7] S. Medici, M. Peana, V.M. Nurchi, J.I. Lachowicz, G. Crisponi, M.A. Zoroddu, Coord. Chem. Rev., vol. 284, 2015, pp. 329–350.

[8] A. Kumar, A. Mitra, A.K. Ajay, M.K. Bhat, C.P. Rao, J. Chem. Sci., vol. 124, 2012, pp. 1217-1228.

[9] S. Gama, I. Rodrigues, F. Mendes, I.C. Santos, E. Gabano, B. Klejevskaja, J. Gonzalez-Garcia, M. Ravera, R. Vilar, A. Paulo, J. Inorg. Biochem., vol. 160, 2016, pp. 275-286.

[10] Q. Yu, Y. Liu, J. Zhang, F. Yang, D. Sun, D. Liu, Y. Zhou, J. Liu, Metallomics : integrated biometal science, vol. 5, 2013, pp. 222-231.

[11] F. Chandra, P. Kumar, S.K. Tripathi, S. Patra, A.L. Koner, ChemMedChem, vol. 11, 2016, pp. 1410-1414.

[12] L.L. Silver, Clin. Microbiol. Rev., vol. 24, 2011, pp. 71-109.

[13] A. Kumar, M. Baumann, J. Balbach, Sci. Rep., vol. 6, 2016, pp. 22533.

[14] J.M. Berg, J. Biol. Chem., vol. 265, 1990, pp. 6513-6516.

[15] J.C. Ebert, R.B. Altman, Protein Sci., vol. 17, 2008, pp. 54-65.

[16] X. Wang, S. Liu, M. Li, P. Yu, X. Chu, L. Li, G. Tan, Y. Wang, X. Chen, Y. Zhang, C. Ning, J. Inorg. Biochem., vol. 163, 2016, pp. 214-220.

[17] V.L. Bodiga, S. Thokala, P.K. Vemuri, S. Bodiga, J. Inorg. Biochem., vol. 153, 2015, pp. 49-59.

[18] R.B. Miguel, P.A. Petersen, F.A. Gonzales-Zubiate, C.C. Oliveira, N. Kumar, R.R. do Nascimento, H.M. Petrilli, A.M. da Costa Ferreira, J. Biol. Inorg. Chem., vol. 20, 2015, pp. 1205-1217.

[19] S.N. Georgiades, L.H. Mak, I. Angurell, E. Rosivatz, M. Firouz Mohd Mustapa, C. Polychroni, R. Woscholski, R. Vilar, J. Biol. Inorg. Chem., vol. 16, 2011, pp. 195-208.

[20] H. Abu Ali, H. Fares, M. Darawsheh, E. Rappocciolo, M. Akkawi, S. Jaber, Eur. J. Med. Chem., vol. 89, 2015, pp. 67-76.

[21] J.P. Chinta, A. Acharya, A. Kumar, C.P. Rao, J. Phys. Chem. B, vol. 113, 2009, pp. 12075-12083.

[22] I. Manet, F. Manoli, M.P. Donzello, E. Viola, A. Masi, G. Andreano, G. Ricciardi, A. Rosa, L. Cellai, C. Ercolani, S. Monti, Inorg. Chem., vol. 52, 2013, pp. 321-328.

[23] N. Raman, R. Mahalakshmi, T. Arun, S. Packianathan, R. Rajkumar, J. Photochem. Photobiol. B, vol. 138, 2014, pp. 211-222.

[24] R.S. Yamgar, Y. Nivid, S. Nalawade, M. Mandewale, R.G. Atram, S.S. Sawant, Bioinorg. Chem. Appl., vol. 2014, 2014, pp. 276598.

[25] X.Q. Zhou, L.B. Meng, Q. Huang, J. Li, K. Zheng, F.L. Zhang, J.Y. Liu, J.P. Xue, ChemMedChem, vol. 10, 2015, pp. 304-311.

[26] J. Shao, Z.Y. Ma, A. Li, Y.H. Liu, C.Z. Xie, Z.Y. Qiang, J.Y. Xu, J. Inorg. Biochem., vol. 136, 2014, pp. 13-23.

[27] M.M. Milutinović, A. Rilak, I. Bratsos, O. Klisurić, M. Vraneš, N. Gligorijević, S. Radulović, Z.D. Bugarčić, J. Inorg. Biochem., vol. 169, 2017, pp. 1-12.

[28] C.A. Bewley, A.M. Gronenborn, G.M. Clore, Annu. Rev. Biophys. Biomol. Struct., vol. 27, 1998, pp. 105-131.

[29] L. Nejdl, B. Ruttkay-Nedecky, J. Kudr, S. Krizkova, K. Smerkova, S. Dostalova, M. Vaculovicova, P. Kopel, J. Zehnalek, L. Trnkova, P. Babula, V. Adam, R. Kizek, Int. J. Biol. Macromol., vol. 64, 2014, pp. 281-287.

[30] S. Clancy, Nature Education vol. 1(1), 2008, pp. 41.

[31] H.W. Boucher, G.H. Talbot, J.S. Bradley, J.E. Edwards, D. Gilbert, L.B. Rice, M. Scheld, B. Spellberg, J. Bartlett, Clin. Infect. Dis., vol. 48, 2009, pp. 1-12.

[32] F. Prestinaci, P. Pezzotti, A. Pantosti, Pathog. Glob. Health, vol. 109, 2015, pp. 309-318.

[33] M. Gottschaldt, A. Pfeifer, D. Koth, H. Gorls, H.M. Dahse, U. Mollmann, M. Obata, S. Yano, Tetrahedron, vol. 62, 2006, pp. 11073-11080.

[34] R. Noguchi, A. Hara, A. Sugie, K. Nomiya, Inorg. Chem. Commun., vol. 9, 2006, pp. 355-359.

[35] S. Abuskhuna, J. Briody, M. McCann, M. Devereux, K. Kavanagh, J.B. Fontecha, V. McKee, Polyhedron, vol. 23, 2004, pp. 1249-1255.

[36] B. Coyle, M. McCann, K. Kavanagh, M. Devereux, V. McKee, N. Kayal, D. Egan, C. Deegan, G.J. Finn, J. Inorg. Biochem., vol. 98, 2004, pp. 1361-1366.

[37] I. Tsyba, B.B.K. Mui, R. Bau, R. Noguchi, K. Nomiya, Inorg. Chem., vol. 42, 2003, pp. 8028-8032.

[38] T. Yamaguchi, K. Yokoyama, C. Nakajima, Y. Suzuki, Biosci. Biotechnol. Biochem., 2017, pp. 1-5.

[39] C. Calvori, L. Frontali, L. Leoni, G. Tecce, Nature, vol. 207, 1965, pp. 417-418.

Acknowledgements

Figure legends
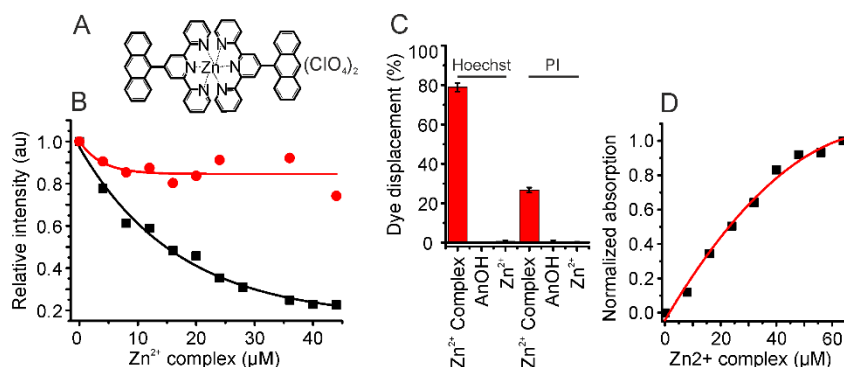
Figure 1. Interaction of the Zn^{2+} complex with DNA. (A) Chemical structure of the Zn^{2+} complex. (B) Relative fluorescence intensity plot of spectral traces obtained during the dye displacement experiment. Red (—) represents propidium iodide and black (—) represents Hoechst 33258. (C) Percentage of dye displacement for the Zn^{2+} complex along with the control molecules. (D) Normalized absorption plot of DNA titrated against Zn^{2+} complex. ■ indiate data point and — shows fitting.
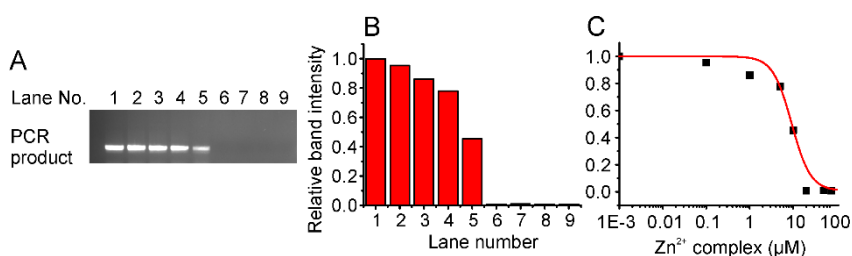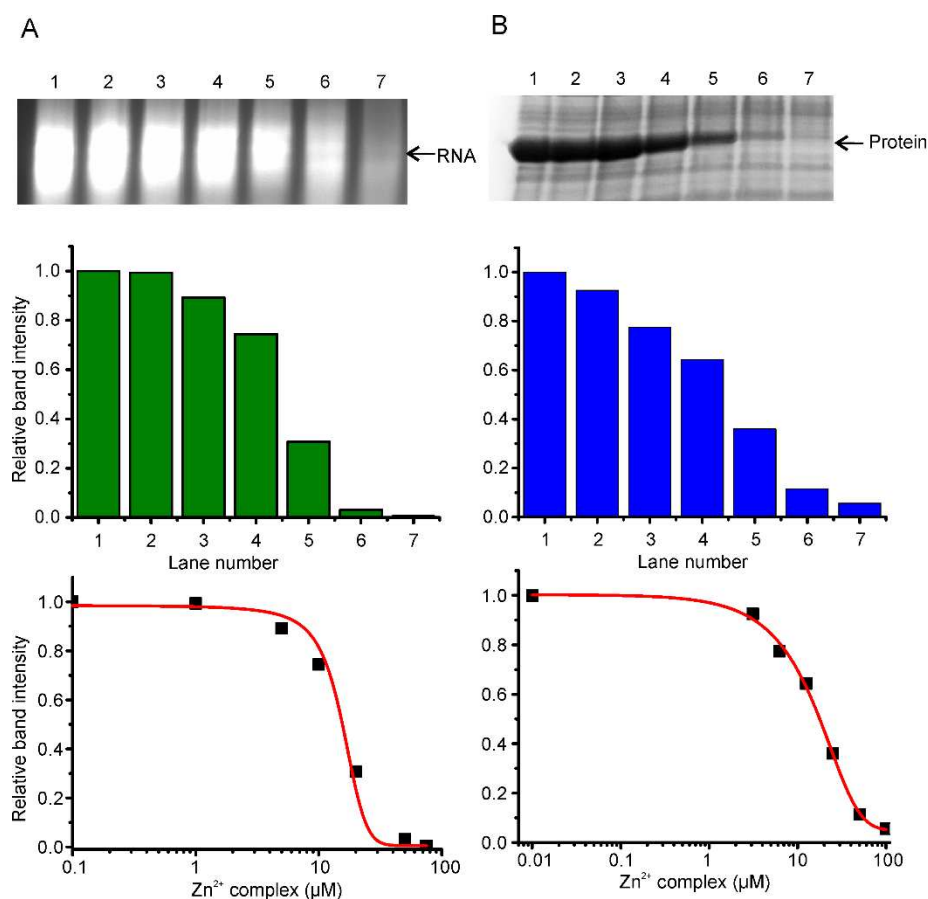

Figure 2: Exhibition of DNA roadblock activity at the DNA level shown by PCR. (A) Agarose gel image indicates the decrease in PCR product with respect to an increasing [Zn^{2+} complex]. Lane 1: control, lane 2: 0.001, lane 3: 1, lane 4: 5, lane 5: 10, lane 6: 20, lane 7: 50, lane 8: 75 and lane 9: 100 µM Zn^{2+} complex. (B) The relative band intensity of each PCR product. (C) The relative band intensity plot (black squares) of (A) and the best fit.
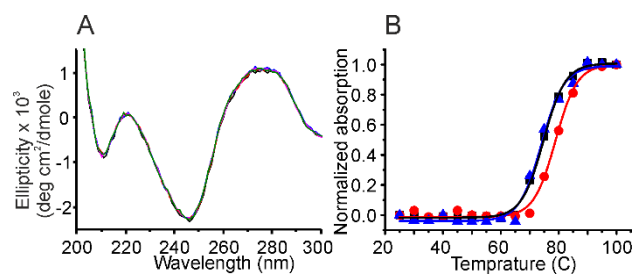
Figure 3: Interaction studies of Zn^{2+} complex with DNA. (A) CD spectral traces of DNA recorded during titration with Zn^{2+} complex. The black DNA spectrum was obtained in the absence of Zn^{2+} complex, while the red, blue, magenta and green spectra were obtained in the presence of an increasing amount of Zn^{2+} complex. (B) DNA melting curves of calf thymus DNA in the absence (■) and presence of Zn^{2+} complex (●) or 9-anthracene methanol (▲).
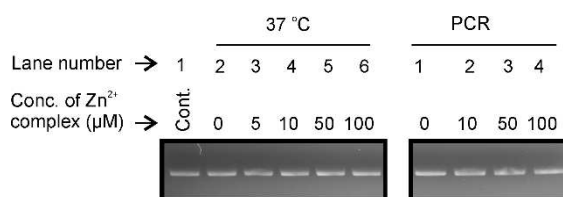
Figure 4: Chemical nuclease activity of the Zn^{2+} complex. (Left) nuclease activity at 37 °C and (right) under PCR conditions.

Figure 5: Exhibition of DNA roadblock activity at the RNA and protein levels (A) Roadblock activity at the RNA level. The top image shows agarose gel analysis of RNA at ~ 500 bases (for p19^{INK4d}). The experiment was performed at the following concentrations; lane 1: 0.1, lane 2: 1, lane 3: 5, lane 4: 10, lane 5: 20, lane 6: 50 and lane 7: 75 µM Zn^{2+} complex. Middle image shows the relative intensity plot of the top image. Bottom image shows the intensity analysis (■) and best fit (red line). (B) Roadblock activity at the protein level. The top image shows the SDS-PAGE analysis of p19^{INK4d} with respect to the [Zn^{2+}complex]. The lanes correspond to following concentrations; Lane 1: 0.01, lane 2: 3.12, lane 3: 6.25, lane 4: 12.5, lane 5: 25, lane 6: 50 and lane 7: 100 µM Zn^{2+} complex. Middle image shows the relative intensity plot of the SDS-PAGE gel. The bottom graph shows the band intensity analysis (■) on top and best fit (red line).
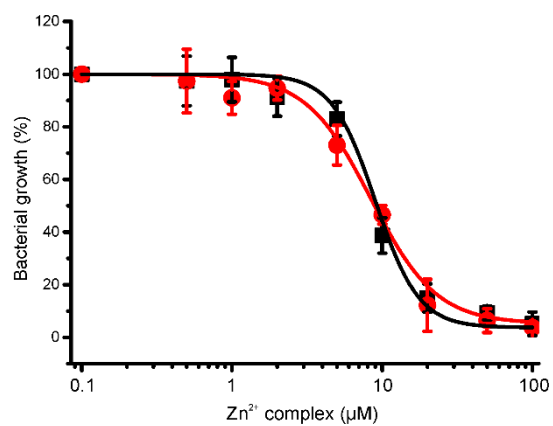
Figure 6: Growth analysis of pathogenic bacteria in the presence of the Zn^{2+} complex. IC_{50} value were determined for Staphylococcus aureus (●) and Pseudomonas aeruginosa (■). Error bars represent mean ± s.d. from triplicate experiments.